Human Hand: Kinematics, Statics and Dynamics

Fai Chen Chen[1], Alain Favetto[2], Mehdi Mousavi[3], Elisa P. Ambrosio[4], Silvia Appendino[5], Alessandro
Battezzato[6], Diego Manfredi[7], Francesco Pescarmona[8], Basilio Bona[9]
Italian Institute of Technology, Center for Space Human Robotics, Corso Trento 21, 10129, Torino, Italy

**The human hand is an extremely complex system due to its large number of degrees
of freedom (DoF) within a significantly reduced space. Moreover, it is required for most
of the tasks performed by humans. That is why it is necessary to understand deeply all
the characteristics of the human hand in order to develop devices interacting with it: to
support it, to substitute injured parts, to help the recovery from injuries, or to enhance
the performances while preserving its natural level of dexterity. The aim of this paper is
to provide a complete and exhaustive summary of the kinematic, static and dynamic
characteristics of the human hand as a preliminary step towards the development of
hand devices such as prosthetic/robotic hands and exoskeletons. Both fields provide
promising opportunities in research and space applications; the former through
humanoid robotic helpers (e.g., Eurobot, Robonaut), the latter through the rising
necessity to help the astronauts during Extravehicular Activity (EVA). In literature,
several papers can be found analyzing kinematics, workspace, constraints and forces of
the human hand[2,4]. However this information is scattered among several papers,
regarding in particular the exerted forces and the dependencies of joint forces and
velocities from the angular values of the same joint or the adjacent one. Direct and
inverse kinematics are presented for all the fingers and the data related to maximum
forces, velocities, acceleration for each joint of each finger has been collected and is
presented in this work.**

I. Introduction

In recent years, as robotics advances, significant efforts have been devoted to the development of hand
devices. The two main application fields related to them are prosthetic/robotic hands and exoskeletons.
Focusing on space applications, there are excellent opportunities for research, the former through humanoid
robotic helpers (e.g., Eurobot, Robonaut) the latter through the rising necessity to help the astronauts during
Extravehicular Activity (EVA) [1] that will be explained with more details in the Section 7.

Some of them present a design with less than 5 fingers[5-7], by which the tasks that can be performed are
limited. Two human fingers can perform 40% of the hand tasks, three fingers can accomplish 90%, and four can
complete 99% of the tasks[8]. This paper is organized as follows: Section 2 presents data about the hand and the
main constraints of the finger movements. Section 3 describes the kinematical model of the hand. Sections 4 to
6 present data about forces, torque, velocities and power. Section 7 discusses how the data presented in this
paper may be used for designing new devices for space applications. Finally, conclusions are presented in
Section 8.

---

[1] PhD Student, Department of Mechanics, Politecnico di Torino, Corso Duca degli Abruzzi 24, 10129, Torino,
Italy

[2] PhD Student, Department of Control and Computer Engineering, Politecnico di Torino, Corso Duca degli
Abruzzi 24, 10129, Torino, Italy.

[3] PhD Student, Department of Mechanics, Politecnico di Torino, Corso Duca degli Abruzzi 24, 10129, Torino,
Italy.

[4] Post-doc researcher, Center for Space Human Robotics, Corso Trento 21, 10129, Torino, Italy.

[5] Post-doc researcher, Center for Space Human Robotics, Corso Trento 21, 10129, Torino, Italy.

[6] Research Assistant, Department of Mechanics, Politecnico di Torino, Corso Duca degli Abruzzi 24, 10129,
Torino, Italy.

[7] Post-doc researcher, Center for Space Human Robotics, Corso Trento 21, 10129, Torino, Italy.

[8] Post-doc researcher, Center for Space Human Robotics, Corso Trento 21, 10129, Torino, Italy.

[9] Department of Control and Computer Engineering, Politecnico di Torino, Corso Duca degli Abruzzi 24,
10129, Torino, Italy

II. Human hand data

The human hand is composed of 5 fingers (Little, Ring, Middle, Index, and Thumb). The thumb is characterized by three articulations (interphalangeal-IP, metacarpophalangeal-MCP and trapeziometacarpal-TMC joints) and three phalanges (Distal Phalanx, Proximal Phalanx and Metacarpal). The other fingers also comprise three different articulations (distal interphalangeal-DIP, proximal interphalangeal-PIP, metacarpophalangeal-MCP joints) and four phalanges (the same phalanges of the thumb plus the middle Phalanx). The wrist has two functional DoFs. The TMC joint of the thumb is characterized by two DoFs (flexion/extension and adduction/abduction) similarly to the MCP joints of the other fingers. A single DoF (flexion/extension) characterizes the MCP and IP joints of the thumb as well as the PIP and DIP joints of the other fingers (Fig. 1). Whereas the eight bones of the carpus articulate finely with each other producing small deformation, the representation into a single rigid segment is a consistent approximation[9].
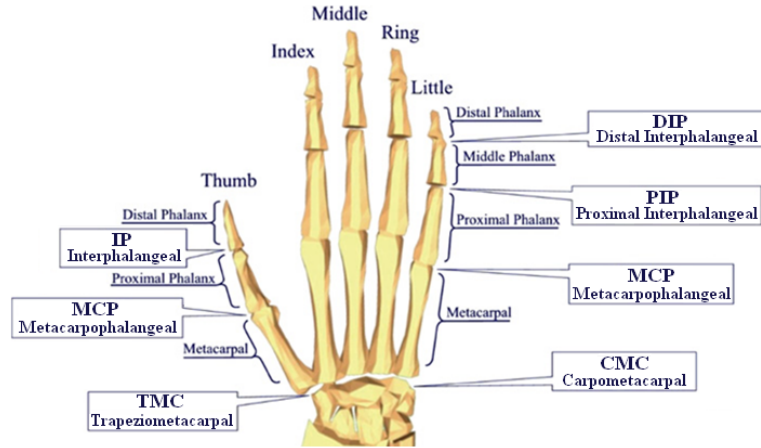

Figure 1. Anatomical details of the hand skeleton.

The analysis of the kinematics, statics and dynamics requires knowledge regarding the dimensions of the fingers and of the palm, and their respective range of motions (ROM): several reports present hand size data. Tables 1 and 2 show the results of Garrett's studies[10,11] for finger lengths and palm dimensions, measurements that were taken from the right hands of 148 men and 211 women. In Table 1, *Crotch to tip* is the distance along the axis of the finger from the midpoint of its tip to the level of the same numbered webbed crotch between two fingers; *Wrist crease to tip* is the distance along the axis of the digit from the midpoint of its tip to the wrist crease baseline.

M	Finger length (crotch to tip)				Finger length (wrist crease to tip[†])			
	mean	s.d.	5%<	95%<	mean	s.d.	5%<	95%<
Thumb	5.87	0.45	5.07	6.57	12.70	1.13	11.05	14.68
Index	7.53	0.46	6.83	8.19	18.52	0.88	17.33	20.06
Middle	8.57	0.51	7.82	9.74	19.52	0.92	18.10	21.04
Ring	8.0	0.47	7.44	8.93	18.72	0.91	17.52	20.28
Little	6.14	0.47	5.44	6.99	16.61	0.91	15.11	18.10
F								
Thumb	5.37	0.44	4.68	6.12	11.05	1.00	9.51	12.83
Index	6.90	0.52	6.10	7.80	16.67	0.89	15.21	18.14
Middle	7.79	0.51	7.01	8.68	17.65	0.87	16.22	19.05
Ring	7.31	0.52	6.52	8.22	16.76	8.94	15.28	18.20
Little	5.46	0.44	4.80	6.24	14.64	0.92	13.11	16.12

Table 1. Mean finger lengths and palm dimensions of USAF male(M)/female(F) flying personnel[10,11] (cm).

Joint		Mean length
Hand length	M	19.72
	F	17.93
Hand breadth	M	8.96
	F	7.71
Hand circumference	M	21.59
	F	18.71
Hand thickness	M	3.29
	F	2.76
Hand depth	M	6.19
	F	5.17

Table 2. Various hand dimensions of USAF male(M)/female(F) flying personnel[10,11] (cm).

A few researchers have measured the length of each phalanx separately. A good study with a variety of candidates is the one achieved by Sahar Refaat[12]. The results of her study for each phalanx of index, middle, ring and little finger are in Table 3 (I1 means distal phalanx, I2 middle phalanx, and I3 proximal phalanx of the index. The same notation is used for the rest of fingers). For another survey we suggest readers to refer also to Jasuja's study[13]. As show in Table 3, the dimensions of the hand are quite similar to the ones presented in Table 2, with a maximum difference of 2.18%. The data presented here is the sample distribution over geographic regions and Air Force Commands, which may be quite representative for EVA glove users.

	Hand	I 1	I 2	I 3	M 1	M 2	M 3	R 1	R 2	R 3	L 1	L 2	L 3
Male Right hand	19.29	2.32	2.37	2.65	2.60	2.78	2.80	2.29	2.56	2.76	1.96	1.92	2.51
Male Left hand	19.36	2.32	2.39	2.61	2.60	2.82	2.75	2.30	2.59	2.78	1.95	1.98	2.49
Female Right hand	17.60	2.23	2.24	2.45	2.44	2.55	2.56	2.12	2.34	2.52	1.79	1.74	2.26
Female Left hand	17.62	2.20	2.24	2.35	2.24	2.43	2.53	2.13	2.36	2.49	1.77	1.77	2.26

Table 3: Mean length of hand and phalanx of index, middle, ring and little finger (cm).

Hand and finger motion is constrained; therefore the natural movements of human fingers are limited to a specific range. Constraints can be roughly divided into three types: static constraints, intra-finger constraints and inter-finger constraints. Intra-finger and inter-finger constraints are often called dynamic constraints, and these are the ones responsible for producing natural movements both statically and dynamically. However, this range of movement is somewhat ambiguous because the range depends on various factors involving human hand biomechanics. The intra-finger constraints are the constraints between joints of the same finger. For instance, $\theta_{DIP} = \frac{2}{3}\theta_{PIP}$. Inter-finger constraints refer to the ones imposed on joints between fingers. For instance, when one bends his index finger at MCP joint, he would naturally have to bend the middle MCP joint as well.

However, there are yet more constraints that cannot be explicitly represented in equations. The normal range of motion of human hand joints corresponds to static constraints on joint angles in the model. These constraints are just limits on the values that the θ parameters can take. Main static constraints (Table 4) have been collected by Cobos[3] et al. Applying these constraints on the inverse kinematics presented on section 3, will reduces the total number of DoFs. Inter-fingers constraints have been defined in Ref. 14.

III. Kinematic model

The kinematic model is composed of 19 links corresponding to the human bones and 24 DoFs modeled by joints. Two kinematic configurations are considered for the hand, one for the thumb, modeled as 3 links and 4 joints and another for the rest of the fingers (index, middle, ring and little), modeled as 4 links and 5 joints, see Figure 2. Note that the CMC joint represents the deformation of the palm, for instance when the hand is grasping a ball, while MCP abduction/adduction is defined before MCP flexion/extension.

A. Direct Kinematics

Direct kinematic equations are used to obtain the fingertip position and orientation according to the joint angles. The model equations are calculated by means of Modified Denavit-Hartenberg (MDH) parameters[15].

Finger	Flexion	Extension	Abduction/ adduction
Thumb			
TMC	50° - 90°	15°	45° - 60°
MCP	75° - 80°	0°	5°
IP	75° - 80°	5° - 10°	5°
Index			
CMC	5°	0°	0°
MCP	90°	30° - 40°	60°
PIP	110°	0°	0°
DIP	80° - 90°	5°	0°
Middle			
CMC	5°	0°	0°
MCP	90°	30° - 40°	45°
PIP	110°	0°	0°
DIP	80° - 90°	5°	0°
Ring			
CMC	10°	0°	0°
MCP	90°	30° - 40°	45°
PIP	120°	0°	0°
DIP	80° - 90°	5°	0°
Little			
CMC	15°	0°	0°
MCP	90°	30° - 40°	50°
PIP	135°	0°	0°
DIP	90°	5°	0°

Table 4. Statics Constraints[3].

1. Direct Kinematics of the index, middle, ring and little finger
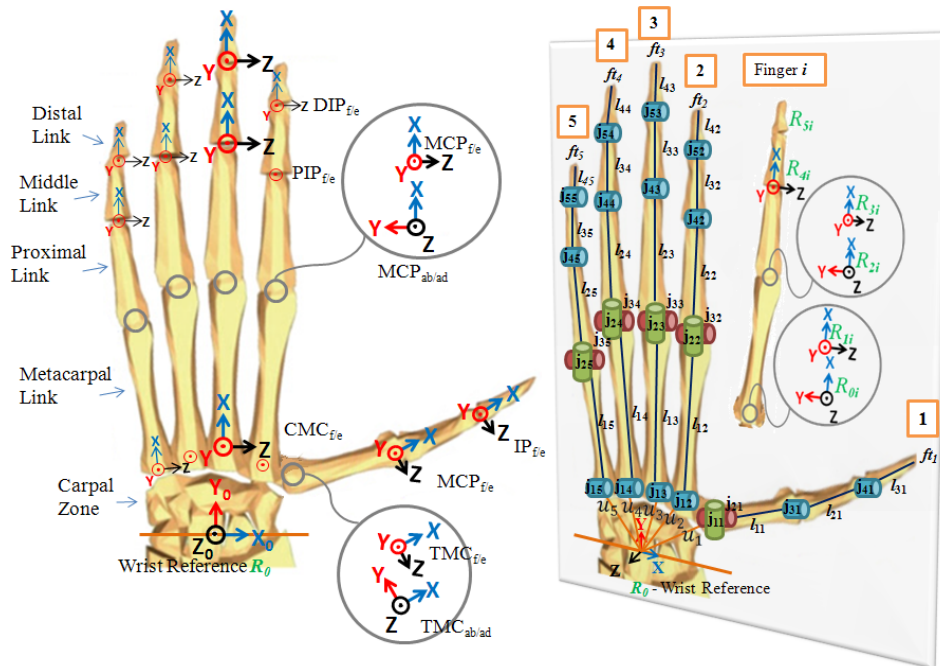

Figure 2. Kinematic configuration of the human hand. Thumb is defined by 3 links and 4 degrees of freedom whereas index, middle, ring and little are defined by 4 links and 5 DoFs.

Each of the fingers presents four bones: metacarpal, proximal, middle and distal (Fig. 1). These bones correspond approximately to the length of each link of the serial kinematic chain (Fig. 2). Each articulation presented above for these four fingers corresponds to the joints: CMC, MCP, PIP, and DIP. The MCP joint presents 2 DoFs realizing the adduction/abduction and flexion/extension movements. The rest of the joints only allow flexion/extension movements. Table 5 shows the MDH parameters for the index finger, which are similar to those of the other fingers except the thumb.

Joint	α_{i-1}	a_{i-1}	d_i	θ_i
j_{12}	$\pi/2$	0	0	$\theta_{CMC_{f/e}}$
j_{22}	$-\pi/2$	L_{12}	0	$\theta_{MCP_{ab/ad}}$
j_{32}	$\pi/2$	0	0	$\theta_{MCP_{f/e}}$
j_{42}	0	L_{22}	0	$\theta_{PIP_{f/e}}$
j_{52}	0	L_{32}	0	$\theta_{DIP_{f/e}}$

Table 5. Modified D-H parameters of the index finger.

Equation 1 shows the direct kinematics from index to little fingers.

$$A_i = {}^{0}_{0i}T \cdot {}^{0i}_{6i}T_i(\theta_{ji}) = {}^{0}_{0i}T \cdot {}^{0i}_{1i}T_i(\theta_{CMC_{f/e}}) \cdot {}^{1i}_{2i}T_i(\theta_{MCP_{ab/ad}}) \cdot {}^{2i}_{3i}T_i(\theta_{MCP_{f/e}}) \cdot {}^{3i}_{4i}T_i(\theta_{PIP_{f/e}}) \cdot {}^{4i}_{5i}T_i(\theta_{DIP_{f/e}}) \cdot {}^{5}_{6}T_{ft_i} \quad (1)$$

Where:

- A_i represents a matrix containing position and orientation of the fingertip of each finger.
- ${}^{0}_{0i}T$ represents a translation and rotation taking into account the fact that the fingers are slightly fanned out and allowing to pass from the initial base Reference frame (R_0) to the alignment of the *i*-th finger first reference frame (R_{0i}).
- ${}^{0i}_{6i}T_i(\theta_j)$ is a matrix containing the geometrical transformation between the *i*-th finger first reference frame and the *i*-th fingertip (ft$_i$). The matrix is composed of the concatenation of the transformation matrices of each finger link.
- ${}^{(n-1)i}_{ni}T_i(\theta_j)$ is a matrix containing the geometrical transformation between the *(n-1)*-th reference frame and the *n*-th reference frame of the *i*-th finger. In particular,
- ${}^{5}_{6}T_{ft_i}$ represents the position of the fingertip with respect to the distal (5th) reference frame.

i corresponds to index(2), middle(3), ring(4) and little(5) finger.
j corresponds to each finger's joint $CMC_{f/e}$, $MCP_{ab/ad}$, $MCP_{f/e}$, $PIP_{f/e}$, $DIP_{f/e}$.
n goes from 0 to 6 from each finger.
ft fingertip of *i*-th finger.

2. Direct Kinematics of the thumb

The thumb presents three bones (Fig. 1): metacarpal, proximal, and distal. These bones correspond approximately to the length of each link. The respective joints are: TMC, MCP, and IP. The TMC joint presents 2 DoFs, allowing adduction/abduction and flexion/extension. Table 6 shows the MDH parameters; equation 2, with the same notation scheme as equation 1, shows the direct kinematics for the thumb.

Joint	α_{i-1}	a_{i-1}	d_i	θ_i
j_{11}	0	0	0	$\theta_{TMC_{ab/ad}}$
j_{21}	$\pi/2$	0	0	$\theta_{TMC_{f/e}}$
j_{31}	0	L_{11}	0	$\theta_{MCP_{f/e}}$
j_{41}	0	L_{21}	0	$\theta_{IP_{f/e}}$

Table 6. Modified D-H parameters of the thumb.

$$A_{thumb} = {}^{0}_{0_{thumb}}T \cdot {}^{0thumb}_{1}T_{thumb}(\theta_k) =$$
$${}^{0}_{0}T \cdot {}^{0}_{1}T_{thumb}(\theta_{TMC_{ab/ad}}) \cdot {}^{1}_{2}T_{thumb}(\theta_{TMC_{f/e}}) \cdot {}^{2}_{3}T_{thumb}(\theta_{MCP_{f/e}}) \cdot {}^{3}_{4}T_{thumb}(\theta_{IP_{f/e}}) \cdot {}^{4}_{5}T_{ft_{thumb}} \quad (2)$$

k corresponds to the thumb joint $TMC_{ab/ad}$, $TMC_{f/e}$, $MCP_{f/e}$, $IP_{f/e}$.

B. Inverse Kinematics

Inverse kinematics is used to obtain the joint angle values according to the fingertip position and orientation. The inverse kinematics will be solved for the index finger and the thumb, as it is almost identical for the other fingers. The model of the human hand is a redundant case; therefore several solutions exist, so to solve the redundant case properly, constraints (Section 2) have been presented to have a convergent solution.

1. Inverse Kinematics of the index.

The angles $\theta_{CMC_{f/e}}$, $\theta_{MCP_{ab/ad}}$, $\theta_{MCP_{f/e}}$, $\theta_{PIP_{f/e}}$, $\theta_{DIP_{f/e}}$ are obtained from equation 1, where the matrix A_2 and the first element are known, based on this algebraically, we solved for the joint $CMC_{f/e}$, $MCP_{ab/ad}$, $DIP_{f/e}$, A_{ij} are the elements of the i-th row and j-th column of the A_2, know for each finger. :

$$\theta_{CMC_{f/e}} = atan\left(\frac{A_{33}}{A_{13}}\right) \quad (3) \ ; \qquad \theta_{MCP_{ab/ad}} = atan\left(\frac{A_{13}}{-A_{13}cos(\theta_{CMC})}\right) \quad (4)$$

$$m = s_2c_3c_4 - s_2s_3s_4 \ ; \quad n = s_2c_3s_4 - s_2s_3c_4 \ ; \quad \epsilon_1 = \frac{(-1).(mA_{22}+nA_{21})}{(m^2-n^2)} \ ; \quad \epsilon_2 = \frac{A_{21}}{m} + \frac{n}{m}.\frac{(-1).(mA_{22}+nA_{21})}{(m^2-n^2)} \quad (5)$$

Where $s_2 = \sin\theta_2$ and so on for the rest, taking into account that $\theta_2 = \theta_{MCP_{ab/ad}}$; $\theta_3 = \theta_{MCP_{f/e}}$ and $\theta_4 = \theta_{PIP_{f/e}}$.

$$\theta_{DIP_{f/e}} = atan2[\epsilon_1, \epsilon_2] \quad (6)$$

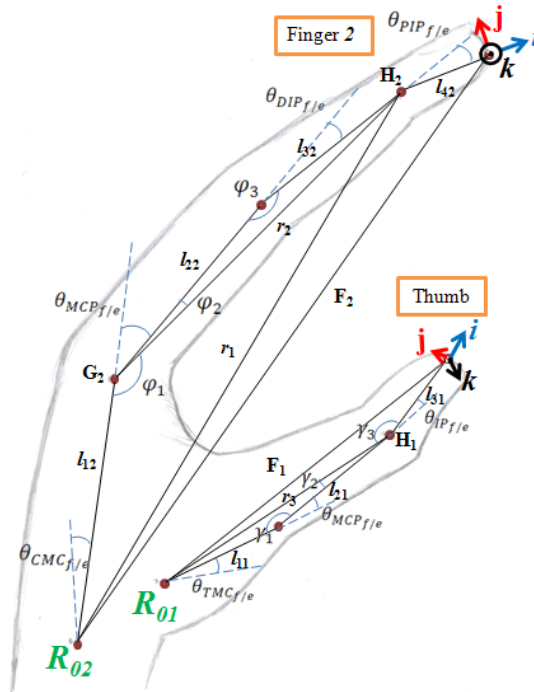The joints $MCP_{f/e}$, $PIP_{f/e}$ are solved through a geometric method, see Fig. 3.

Figure 3. Inverse Kinematics for the index finger and thumb.

Starting from the vector $\overrightarrow{F_2}$ which contains the position of the fingertip, it is possible to obtain $\overrightarrow{H_2}$ with the following expression:

$$\overrightarrow{H_2} = \overrightarrow{F_2} - [l_{42} * \hat{\imath}] \quad (7)$$

The vector $\overrightarrow{G_2}$ is calculated as:

$$\overrightarrow{G_2} = [G_{2x} \ G_{2y} \ G_{2z}]^T \ ; \quad G_{2x} = l_{12}cos(\theta_{CMC}) \ ; \quad G_{2y} = l_{12}sin(\theta_{CMC}) \ ; \quad G_{2z} = 0 \quad (8)$$

The vector $\overrightarrow{u_2}$, and the values s_1 and s_2 are obtained using the already calculated $\overrightarrow{H_2}$ and $\overrightarrow{G_2}$:

$$\overrightarrow{u_2} = \overrightarrow{H_2} - \overrightarrow{G_2} \ ; r_1 = \|\overrightarrow{H_2}\| \ ; r_2 = \|\overrightarrow{u_2}\| \ ; \varphi_1 = acos\left(\frac{r_2^2+l_{12}^2-r_1^2}{2r_2l_{12}}\right) \ ; \varphi_2 = acos\left(\frac{r_2^2+l_{22}^2-l_{32}^2}{2r_2l_{22}}\right) \quad (9)$$

American Institute of Aeronautics and Astronautics

MCP flexion/extension is obtained as:

$$\theta_{MCP_{f/e}} = \pi - \varphi_1 - \varphi_2 \qquad (10)$$

PIP flexion/extension is obtained as:

$$\varphi_3 = acos\left(\frac{l_{32}{}^2 + l_{22}{}^2 - r_2{}^2}{2l_{32}l_{22}}\right); \qquad \theta_{PIP_{f/e}} = \pi - \varphi_3 \qquad (11)$$

2. Inverse Kinematics of the thumb

The same procedure can be applied to the thumb, in which A_{Thumb} and the first element of equation 2 are also known, the joint $TMC_{ab/ad}$ is obtained algebraically as follows:

$$\theta_{TMC_{ab/ad}} = atan\left(\frac{A_{13}}{-A_{23}}\right) \qquad (12)$$

By the geometry method the joints $MCP_{f/e}$, $IP_{f/e}$ are obtained as follows (Fig. 3),

$$\overrightarrow{H_1} = \overrightarrow{F_1} - [l_{31} * \hat{\imath}]; \qquad r_3 = \|\overrightarrow{H_1}\|; \qquad r_4 = \|\overrightarrow{F_1}\| \qquad (13)$$

$$\gamma_1 = acos\left(\frac{l_{21}{}^2 + l_{11}{}^2 - r_3{}^2}{2l_{21}l_{11}}\right); \qquad \gamma_2 = acos\left(\frac{l_{31}{}^2 + s_3{}^2 - r_4{}^2}{2l_{31}r_3}\right); \qquad \gamma_3 = acos\left(\frac{r_3{}^2 + l_{21}{}^2 - l_{11}{}^2}{2r_s l_{21}}\right) \qquad (14)$$

$$\theta_{MCP_{f/e}} = \pi - \gamma_1 ; \qquad \theta_{IP_{f/e}} = \pi - \gamma_2 - \gamma_3 \qquad (15)$$

The joint $\theta_{TMC_{f/e}}$ is obtained algebraically as follows:

$$\mu = \theta_{MCP} + \theta_{IP} ; \qquad \epsilon_3 = (A_{32} + A_{31})\cos\mu ; \qquad \epsilon_4 = \frac{A_{31} - (A_{31} + A_{32})\cos\mu . \sin\mu}{\cos\mu} \qquad (16)$$

$$\theta_{TMC_{f/e}} = atan2[\epsilon_4, \epsilon_3] \qquad (17)$$

IV. Force and torque

An understanding of the capabilities of the human hand provides a basis for the development of an exoskeleton for enhancing astronaut's hand performance while wearing the EVA glove, as described in Section 7. Forces normal to each phalanx (bone) of each finger in a cylindrical power grasp (Fig. 4a) were recorded by An[16], et al. The apparatus allowed recording strain gage measurements at the mid-point of each phalange; a summary of these measurements appears in Table 7. These values can give us a clearer image of which is the range of force when a particular task is performed.
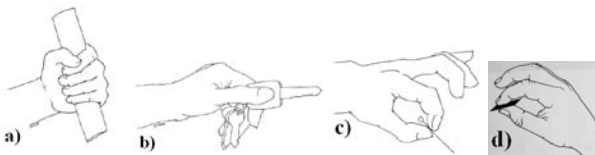

Figure 4. Grasps. *a) Cylindrical power grasp*[17]*, b) Key pinch grasp*[17]*, c) Tip pinch*[17]*, d) Palmar pinch (pulp pinch).*

	Proximal	Middle	Distal
Index	42	22	62
Middle	24	40	68
Ring	15	28	44
Little	7	20	31

Table 7: Maximun mid-phalangeal joint forces exerted by human fingers in a cylindrical power grasp[16] (N).

Another study was performed by Lowe[18], et al. He used a system that incorporated 20 conductive polymer resistance-based force sensors attached to a thin leather athletic grip glove (Fig. 5). The active area of each sensor was circular with a diameter of 9.53 mm. The thickness of each sensor was 0.127 mm. Table 8 shows the average distribution of forces over the 16 finger segments for 24 subjects performing a maximum cylindrical power grip. This study allows us to know how the forces are distributed among certain points of the hand. Single phalanx differences from An's work and Lowe's work are in a range between 0.7% and 25.9%, but proximal phalanx cannot be compared because Lowe's study add also Meta-head distribution.
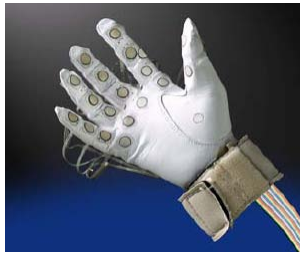
Figure 5. Sensor placement on the force glove[18].

	Proximal	Middle	Distal	Meta-head
Index	21 (4.7%)	26.1 (5.9%)	45.9 (10.4%)	17.3 (3.9%)
Middle	29.3 (6.6%)	36.5 (8.2%)	64.1 (14.5%)	24.2 (5.5%)
Ring	22.3 (5%)	27.8 (6.3%)	48.8 (11%)	18.4 (4.2%)
Little	11.6 (2.6%)	14.5 (3.3%)	25.4 (5.7%)	9.6 (2.2%)

Table 8. The average distribution of forces. Values are in Newton (N) and percentage of total force[18].

Finger abduction and adduction force capabilities have also been studied. An et al. measured maximum abduction forces between the index and the middle finger of 40N, and adduction forces of slightly over 30N. Also the lateral strength of the index finger and thumb (Table 9). The thumb appears to be by far the most powerful of the digits, a clear case can be seen in Table 9, where the typical key pinch (Fig. 4*b*) strength for males as 109N, more than twice as Sutter's[25] maximum of 50N at the index fingertip. An's 75N measurement of thumb ulnar deviation is also much higher than any finger abduction/adduction measurement. Another study made by Kroemer and Gienapp[19] provides results which confirm An's result. Kroemer and Gienapp did the same study for 31 male Air Force pilots. The average thumb tip forces range from 84 N for the "thumbs up" position to 99 N for the key pinch position with the thumb MCP joint fully flexed[19].

	Tip	Pulp	Key	Radial Deviation		Ulnar deviation	
	Pinch	Pinch	Pinch	Thumb	Index	Thumb	Index
Male	65	61	109	43	43	75	42
Female	45	43	76	25	31	43	28

Table 9. Normal hand strength[16] (N).

A different study was carried out by Astin[20]. Table 10 shows the summary and comparison of mean strength in key pinch, palmar pinch and power grip for males and females subjects in Mathiowetz[21], Imrhan[22] and Astin studies.

Bretz[23], et al has also performed some study to measure the fingers forces. Table 11 shows the results. These studies confirm previous work.

Mean Strength	Astin Results	Mathiowetz Results	Imrhan Results
key pinch (Fig. 4*b*)			
Male	97	110	92
Female	65	73	64
Palmar pinch (Fig. 4*d*)			
Male	63	76	72
Female	45	51	46
Power grip (Fig. 4*a*)			
Male	452	466	487
Female	289	280	308

Table 10. The summary and comparison of mean strength in lateral pinch, palmar pinch and power grip for males and females subjects in Mathiowetz, Imrhan and Astin studies (N).

	Average Force Measurement					
	Hand	Little	Ring	Middle	Index	Thumb
Rigth hand	551	31	38	55	57	108
Left hand	505	28	37	54	60	109

Table 11. Results of Bertz's study (N).

Assuming representative phalangeal lengths and joint angles for the hand in a cylindrical grasp, joint torques corresponding to the above forces were calculated (Table 12). The force vectors were calculated as follows, where θ is the joint angle[24], taking into account Fig. 6.

	MCP	PIP	DIP
Index	270	228	77.5
Middle	322	289	85
Ring	203	180	55
Little	126	120	39.8

Table 12. Joint torques exerted by human fingers in cylindrical grasp (Ncm).

	MCP	PIP	DIP
Index	463	213	62.5
Middle	500	225	62,.5
Ring	370	170	50
Little	N/A	N/A	N/A

Table 13. Joint torques exerted by human fingers in fingertip force test[24] (Ncm).

$$l_i = l_i \cos\left(\sum_{j=1}^{i} \theta_j\right) i + l_i \sin\left(\sum_{j=1}^{i} \theta_j\right) j \qquad (18)$$

$$f_i = f_i \cos\left(\pi + \sum_{j=1}^{i} \theta_j\right) i + f_i \sin\left(\pi + \sum_{j=1}^{i} \theta_j\right) j \qquad (19)$$

The joint torques can then be calculated:

$$\tau_1 = \frac{l_1}{2} f_1 + \left(l_1 + \frac{l_2}{2}\right) f_2 + \left(l_1 + l_2 + \frac{l_3}{2}\right) f_3 \qquad (20)$$

$$\tau_2 = \frac{l_2}{2} f_2 + \left(l_2 + \frac{l_3}{2}\right) f_3 \qquad (21)$$
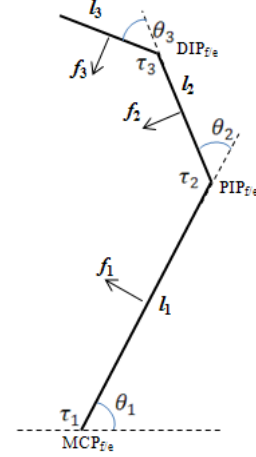
$$\tau_3 = \frac{l_3}{2} f_3 \qquad (22)$$

Figure 6. Vector diagram for finger with mid-phalangeal forces[24].

Another study was performed by Sutter[25], et al. The study reported 50Nas the maximum force exerted at the tips of human index and middle fingers, and 40N for the ring finger. The same approach used to calculate joint torques in a cylindrical grasp has been used to calculate the joint torques from Sutter's fingertip force data, unlike An, et al. Sutter measured maximum fingertip forces with the fingers fully extended, so all angles are zero in the torque calculation (Table 13). An interesting fact is that Sutter observed that maximum joint torque is roughly independent from MCP joint angle for the angles in question. Though Sutter and An's data were obtained under different circumstances, a cautious comparison is useful to determine the maximum of the human hand capabilities due to the fact that actuator dimensioning for hand exoskeletons or similar applications may be done according to this data, to obtain the same range of force. Hasser[24] concludes that An's cylinder experiment did not fully challenge the MCP joint, but it challenged the PIP and DIP joints more than Sutter's, in the

	MCP	PIP	DIP
Index	463	228	77.5
Middle	500	289	85.0
Ring	370	180	55.0
Little	N/A	120	39.8

Table 14. Maximum torque capabilities of human finger joints[24] (Ncm).

contrary Sutter's experiment challenged the MCP joint, but not the PIP and DIP joints; so we can merge both An and Sutter's studies that provide us the maximum joint torques (Table 14). Future work should comprise experiments on different hand movements, to obtain a thorough knowledge of maximum forces.

V. Velocities

Little information exists on maximum velocities of finger joints or representative velocities during task completion. Maximum velocities would be useful as an upper bound for no-load velocities of force-reflecting hand masters. Knowledge of maximum velocities can also contribute to estimate the human joint power capability in the absence of coordinated force and velocity measurements. Knowledge of actual joint velocities during typical hand tasks would also be useful for determining system requirements.

Darling[26], et al. measured MCP and PIP joints velocities while studying the finger dynamics of four subjects [22]. The maximum MCP velocity measured by one of the subjects corresponds to 18 rad/s and maximum PIP velocity of 12 rad/s. Darling[27] states that the velocities seem to range as high as 20 rad/s. Darling[26], cites a peak PIP velocity of 10 rad/s for "natural velocity" movement in the PIP joint and a range of 3-6 rad/s for the MCP and PIP joints in "slow" motion.

The experimental results agree with those of Marcus[28], et al. at EXOS that reported a maximum MCP joint velocity averaged across the four male subjects of 17 rad /s. A brief investigation by EXOS engineers yielded similar results. PIP joint velocity was not measured, though the maximum PIP velocity might be estimated at 18 rad/s.

VI. Power

Data from An, et al. and Sutter, et al. contribute to an estimate of maximum human joint power. The maximum MCP joint torque, calculated from Sutter's middle finger data, is 5 Nm. The maximum PIP joint torque, calculated from An's middle finger data, is 2.89 Nm. Linear interpolation between an MCP stall force of 5 Nm and an MCP no-load velocity of 17 rad/s yields 2.5 Nm at 8.5 rad/s for the power calculation (assuming maximum power at half maximum angular velocity and half maximum torque). The calculation for the PIP joint is similar:

MCP joint: (8.5 rad/s) (2.5 Nm) = 21 W

PIP joint: (9.0 rad/s) (1.44 Nm) = 13 W

The above linearly-interpolated calculation assumed maximum power at ½ maximum angular velocity and ½ maximum torque. Hollerbach, et al. show that muscle does not have a linear strain/stress curve, and that maximum power occurs at 1/3 maximum velocity and 1/3 maximum force [24]. This results in the following power estimates for human finger joints:

MCP joint: (5.67 rad/s) (1.67 Nm) = 9.4 W

PIP joint: (6.0 rad/s) (0.96 Nm) = 5.8 W

Stated simply, maximum power of a muscle in this situation would be 0.11 (maximum angular velocity x maximum torque).

VII. Discussion for Space Application

As mentioned above, the human hand is the most important tool for astronauts to perform tasks during an extravehicular activity (EVA): nevertheless, mandatory EVA equipment strongly reduces hand performances, in particular as regards dexterity, mobility and fatigue. Our research group is focusing on the design and development of a lightweight hand exoskeleton, to be worn inside the EVA glove, in order to augment hand performances and counteract the stiffness of the pressurized space suit. The data collected and presented in this paper allows interested researchers to deeply understand the human hand, kinematics, forces of each finger, joint constraints. This will aid in the design of an exoskeleton prototype, as well as other hand device applications, where the main point is to roughly mimic the characteristics of the human hand, for instance the joints' positions, joints' constraints, as well as the DoFs. For applications such as exoskeletons, which must be worn on the human body, the structure should be built to avoid changing the kinematics of the part of the body where it has to be placed. Key factors for the design of an EVA glove hand exoskeleton have been reviewed[30]. Other important space application which may benefit of from data presented in this work is the design of end effectors in rovers and in manipulators, as shown in figure 7.
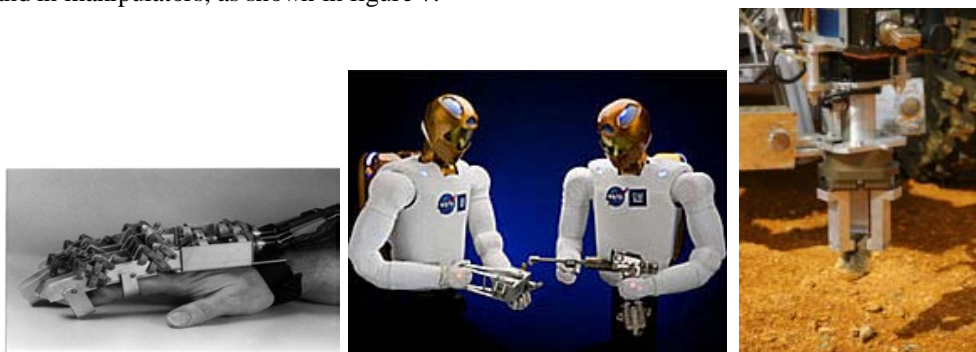

Figure 7. Space applications. *a) An anthropomorphic hand exoskeleton to prevent astronaut hand's fatigue during extravehicular activities[31], b) Robonaut's hand as end effector[32] c) Eurobot Ground Prototype end effector[33].*

VIII. Conclusions an future work

This work aims at providing a complete review of the kinematics, statics and dynamics of the human fingers such that it will provide the basis for both the development of future comparative studies as well as future projects related to human hands. Collected data will be applied for the development of a hand exoskeleton for an EVA glove, but may be useful for all projects comprising devices which must interact with or emulate the human hand.

References

[1] Jordan, N., Saleh, J., Newman, D., "The extravehicular mobility unit: A review of environment, requirements, and design changes in the US spacesuit," Acta Astronautica 59, 2006, pp. 1135-1145.

[2] Leijnse, J., Quesada, P., Spoor, C., "Kinematic evaluation of the finger's interphalangeal joints coupling mechanism - variability, flexion - extension differences, triggers, locking swanneck deformities, anthropometric correlations," Journal of Biomechanics 43, 2010, pp. 2381-2393.

[3] Cobos, S., Ferre, M., Sanchez, M., Ortegom, J., Peña, C., "Efficient Human Hand Kinematics for Manipulation Tasks," IEEE/RSJ International Conference on Intelligent Robots and Systems Acropolis Convention Center. Nice, France, September 22-26, 2008.

[4] Lin, J., Wu, Y., Huang, T., "Modeling the Constraints of Human Hand Motion," Proceedings workshop on human motion, 2000, pp. 121-126.

[5] Fontana, M., Dettori, A., Salsedo, F., and Bergamasco, M., "Mechanical design of a novel Hand Exoskeleton for accurate force displaying," Kobe International Conference Center, May 12-17, 2009.

[6] Imamura, N., Kaneko, M., Tsuji, T., "Development of Three-Fingered Robot Hand with a New Design Concept," Robotics and Manufacturing, July 26-29, 1998.

[7] Jau, B., "Dexterous telemanipulation with four fingered hand system," IEEE International Conference on Robotics and Automation, 1995.

[8] Mishkin, A. H., and Jau, B. M., "Space-Based Multifunctional End Effector Systems: Functional Requirements and Proposed Designs," Technical Report 88-16, NASA JPL, Pasadena, California, April 1988.

[9] Cerveri, P., Lopomo, P., Pedotti, A., and Ferrigno, G., "Derivation of Centers and Axes of Rotation for Wrist and Fingers in a Hand Kinematic Model: Methods and Reliability Results," Annals of Biomedical Engineering, Vol. 33, No. 3, March 2005, pp. 402-412,.

[10] Garrett, J. W., "Anthropometry of the hands of male air force flight personnel," Technical report, Aerospace medical research laboratory, Air Force systems command, Wright-Patterson Air Force Base, Ohio, 1970.

[11] Garrett, J. W., "Anthropometry of the hands of female air force flight personnel," Technical report, Aerospace medical research laboratory, Air Force systems command, Wright-Patterson Air Force Base, Ohio, 1970.

[12] Habib, S. R., Kamal, N. N., "Stature estimation from hand and phalanges lengths of Egyptians," Journal of Forensic and Legal Medicine, Volume 17, Issue 3, April 2010, PP. 156-160.

[13] Jasuja, O. P., singh, G., "Estimation of stature from hand and phalange length," Journal of Indian Academy of Forensic Medicine, Volume 26, Issue 3, 2004.

[14] Cobos, S., Ferre, M., Sanchez-Uran, M.A., and Ortego, J., "Constraints for Realistic Hand Manipulation," The 10th Annual International Workshop on Presence, October 25 - 27 Barcelona, Spain, 2007, pp. 369-370.

[15] Craig, J. J., "Introduction to Robotics, Mechanics and Control," Pearson Education International, Third edition, 1986, pp. 67-76.

[16] An, K. N., Askew, L., and Chao, E.Y., "Biomechanics and Functional Assessment of Upper Extremities," In W. Karwowski, editor, Trends in Ergonomics/Human Factors III, 1986, pp. 573-580.

[17] Lippert, L. S., "Clinical Kinesiology and Anatomy," F. A. Davis Company, 4th edition, 2006, pp. 161-164.

[18] Lowe, B. D., Kong, Y., and Han, J., "Development and application of a hand force measurement system," Proceedings of the XVIth Triennial Congress of the International Ergonomics Association, 2006.

[19] Kroemer, K. H. E., and Gienapp, E. M., "Hand-Held Device to Measure Finger (Thumb) Strengh," Journal of Applied Physiology, vol. 29 no. 4, October 1970, pp. 526-527.

[20] Astin, A. D., "Finger force capability: measurement and prediction using anthropometric and myoelectric measures," Master of Science Thesis, Faculty of the Virginia Polytechnic Institute and State University, December 16, 1999.

[21] Mathiowetz, V., Kashman, N., Volland, G., Weber, K., Dowe, M., and Rogers, S., "Grip and pinch strength: normative data for adults," Archives of Physical Medicine and Rehabilitation, 1985, pp. 69-74.

[22] Imrhan, S. N., "Trends in finger pinch strength in children, adults, and the elderly," Human Factors, 1989, pp 689-701.

[23] Bretz, K. J., Jobbágy, Á., Bretz, K., "Force Measurement of Hand and Fingers," Biomechanica Hungarica III, 2010, pp 61-66.

[24] Hasser, C. J., "Force-Reflecting Anthropomorphic Hand Masters," Crew Systems Directorate, Biodynamics and Biocommunications Division, Armstrong Laboratory, July 1995, pp. 35-41.

[25] Sutter, P. H., Iatridis, J. C., and Thakor, N. V., "Response to Reflected-Force Feedback to Fingers in Teleoperations," Proceedings NASA Conference on Space Telerobotics, NASA JPL, January 1989, pp. 65-74.

[26] Darling, W. G., and Cole, K. J., "Muscle Activation Patterns and Kinetics of Human Index Finger Movements," J. Neurophysiology, 63(5), May 1990, pp 1098-1108.

[27] Darling, W. G., "Personal Communication," University of Iowa, Iowa City, IA, 1995.

[28] EXOS, Inc, Development of a Force Feedback Anthropomorphic Teleoperation Input Device for Control if Robot Hands, Nasa Phase I SBIR NAS8-38910, EXOS Inc., 8 Blanchard Rd., Burlington, MA 01803, August 1991

[29] Hollerbach, J. M., Hunter, I. W., and Ballantyne, J., "A Comparative Analysis of Actuator Technologies for Robotics," In M. Rahimi and W. Karwowski, editors, The Robotics Review 2, MIT Press, 1991.

[30] Favetto, A., Chen Chen, F., Ambrosio, E. P., Manfredi, D., and Calafiore, G. C., "Towards a Hand Exoskeleton for a Smart EVA Glove," Proceedings of the 2010 IEEE International Conference on Robotics and Biomimetics, China, 2010.

[31] Shields, B. L., Main, J. A., Peterson, S. W., and Strauss, A. M., "An Anthropomorphic Hand Exoskeleton to Prevent Astronaut Hand Fatigue During Extravehicular Activities," IEEE transactions on systems, man, and cybernetics-part A: systems and humans, vol. 27, no. 5, September 1997, pp. 668-673.

[32] What is a Robonaut?, URL: http://robonaut.jsc.nasa.gov/default.asp

[33] Eurobot Ground Prototype, URL: http://www.esa.int/esaHS/SEM9NCZGRMG_research_0.html